

Radiative lifetime of the $a^3\Sigma^+$ state of HeH^+ from *ab initio* calculations

J. Loreau,^{a)} J. Liévin, and N. Vaeck

Laboratoire de Chimie Quantique et Photophysique, Université Libre de Bruxelles,
CP160/09, 50 av. F. D. Roosevelt, 1050 Bruxelles, Belgium

(Received 26 May 2010; accepted 3 August 2010; published online 15 September 2010)

The first metastable triplet state of HeH^+ was found to be present in ion beam experiments, with its lifetime estimated to be between hundreds of milliseconds and thousand of seconds. In this work, we use *ab initio* methods to evaluate the radiative lifetimes of the six vibrational levels of the $a^3\Sigma^+$ of HeH^+ . The transition $a^3\Sigma^+ \rightarrow X^1\Sigma^+$ is spin-forbidden, but acquires intensity through spin-orbit interaction with the singlet and triplet Π states. Large scale CASSCF/MRCI calculations using an adapted basis set were performed to determine the potential energy curves of the relevant states of HeH^+ as well as the matrix elements of the dipole and spin-orbit operators. The wave functions and energies of the vibrational levels of the $a^3\Sigma^+$ and $X^1\Sigma^+$ states are obtained using a B-spline method and compared to previous works. We find that the radiative lifetime of the vibrational levels increases strongly with v , the lifetime of the $v=0$ state being 150 s. We also analyze the contributions from discrete and continuum parts of the spectrum. With such a long lifetime, the $a^3\Sigma^+$ state could have astrophysical implications. © 2010 American Institute of Physics. [doi:10.1063/1.3481782]

I. INTRODUCTION

The helium hydride ion HeH^+ is one of the most elementary molecular ions and the first to form in the early universe.¹ Due to its high relative abundance, HeH^+ was predicted to be observable in astrophysical objects such as planetary and gaseous nebulae,² or in metal-poor stars.³ However, no infrared emission from HeH^+ molecular ion has yet been detected from these objects,^{4,5} although it has been observed in laboratory plasmas for many years.⁶ The formation of HeH^+ is mainly due to the radiative association between He and H^+ or between He^+ and H.⁷ While it was always supposed that HeH^+ formed in its ground $X^1\Sigma^+$ state, one should also consider the possible role of the first metastable triplet state, $a^3\Sigma^+$. This state can indeed be populated and will not decay by collisions if the plasma density is low. As its radiative decay to the ground state is spin-forbidden, it is thus expected to have a very long lifetime.

In studies on the dissociative recombination of HeH^+ , it was shown that the $a^3\Sigma^+$ state is responsible for a part of the cross section, so that it must be present in the ion beam. The lifetime of this state was postulated by Yousif *et al.*⁸ to be longer than the one of $\text{He}(1s2s^3S)$, which decays by a relativistic magnetic dipole transition and has a lifetime of approximately 8000 s. In an experiment on the charge-transfer dissociation of HeH^+ , Strasser *et al.*⁹ estimated the lifetime of the triplet state to be in the range of a few hundreds of milliseconds, a much lower value probably due to collisional decay. These two estimations provide lower and upper bounds on the lifetime of this state, but the difference is so large that it motivates a theoretical investigation of the lifetime.

We present in this work the results of large scale

ab initio calculations performed with the MOLPRO program suite.¹⁰ These calculations take the spin-orbit coupling between the low-lying singlet and triplet Σ^+ and Π states into account, allowing the spin-forbidden $a^3\Sigma^+ \rightarrow X^1\Sigma^+$ dipole transition to occur. This mechanism was already used to estimate the lifetime of the first triplet state of NO^+ .^{11,12}

The resolution of the vibrational problem in the considered potential energy curves has been done using a B-spline basis set method, which allowed us to estimate the contribution of the continuum states to the lifetime.

II. THEORY

A. Lifetime

The inverse of the lifetime τ_i of an initial excited electronic state $|i\rangle$ is given in the electric dipole approximation by¹³

$$\tau_i^{-1} = \sum_f A_{if} = \frac{4}{3\hbar^4 c^3} \sum_f E_{if}^3 |\langle i | \boldsymbol{\mu} | f \rangle|^2, \quad (1)$$

where the sum extends over all states $|f\rangle$ with an energy $E_f < E_i$. The A_{if} are the so-called Einstein coefficients for spontaneous emission and $\boldsymbol{\mu}$ is the dipole operator. $E_{if} = E_i - E_f$ is the energy difference between states $|i\rangle$ and $|f\rangle$.

In the Born–Oppenheimer approximation, the total wave function for the initial or the final state is expanded as a product of electronic, vibrational, and rotational wave functions. These three types of motions are represented by the quantum numbers m (electronic), v (vibrational), and J (rotational). In Hund's case (a), the wave function for a state $|mvJ\rangle$ is

^{a)}Electronic mail: jloreau@ulb.ac.be.

$$\Psi_{mvJ} = \zeta_{m\Lambda\Sigma}(R, r) \psi_{mvJ\Lambda\Sigma}(R) \bar{D}_{M\Omega}^J(\theta, \phi). \quad (2)$$

Λ is a quantum number associated to L_z , the projection on the internuclear z axis of the total electronic angular momentum \mathbf{L} . Σ is associated to S_z , the projection on the z axis of the total electronic spin \mathbf{S} . The total angular momentum is $\mathbf{J} = \mathbf{N} + \mathbf{L} + \mathbf{S}$, where \mathbf{N} is the angular momentum for nuclear rotation. $\Omega = \Lambda + \Sigma$ is a quantum number associated with J_z . The vibrational equation that the functions $\psi_{mvJ\Lambda\Sigma}(R)$ must satisfy is, in atomic units,

$$\left(-\frac{1}{2\mu} \partial_R^2 + U_{mvJ\Lambda\Sigma}(R) - E_{mvJ\Lambda\Sigma} \right) \psi_{mvJ\Lambda\Sigma}(R) = 0, \quad (3)$$

where $U_{mvJ\Lambda\Sigma}(R)$ is the electronic energy, $U_{m\Lambda\Sigma}(R)$, corrected by a centrifugal term originating from the rotational Hamiltonian,

$$U_{mvJ\Lambda\Sigma}(R) = U_{m\Lambda\Sigma}(R) + \frac{1}{2\mu R^2} (J(J+1) - \Omega^2 + S(S+1) - \Sigma^2), \quad (4)$$

and μ is the reduced mass of the system. Note that the diagonal Born–Oppenheimer corrections, as well as nonadiabatic and relativistic corrections other than the spin-orbit interaction, have been omitted.

If we neglect the rotational motion (that is, we average over the initial states and neglect the energy dependence of rotational states), the dipole transition moment between the initial and the final states is then given by

$$\langle iv | \boldsymbol{\mu} | fv' \rangle = \langle iv \Lambda S | \langle i \Lambda S \Sigma | \boldsymbol{\mu} | f \Lambda' S' \Sigma' \rangle | fv' \Lambda' S' \rangle, \quad (5)$$

while the lifetime of the vibrational level v of the excited electronic state i is given by

$$\tau_{iv}^{-1} = \sum_f \sum_{v'} A_{iv, fv'}, \quad (6)$$

where the Einstein coefficients $A_{iv, fv'}$ are

$$A_{iv, fv'} = \frac{4}{3\hbar^4 c^3} E_{iv, fv'}^3 |\langle iv \Lambda S | \langle i \Lambda S \Sigma | \boldsymbol{\mu} | f \Lambda' S' \Sigma' \rangle | fv' \Lambda' S' \rangle|^2. \quad (7)$$

To be exact, the sum over the vibrational levels v' of state f in Eq. (6) should be understood as a sum if v' is a discrete (bound) level or as an integral if v' is a continuum (unbound) level. However, as explained below, we will use a discretization method to treat the continuum, so that the sum will run over the discrete levels until convergence in Eq. (6). As the ground state is the only state below the $a^3\Sigma^+$ state, the sum over f will reduce to only one term.

To calculate the lifetime of state $|i\rangle$, it is thus necessary to know (i) its transition moments with all the states $|f\rangle$ lower in energy, and (ii) the vibrational wave functions (and energies) of states $|i\rangle$ and $|f\rangle$.

B. Spin-orbit coupling

The transition $a^3\Sigma^+ - X^1\Sigma^+$ is forbidden at all multipole orders due to the spin selection rule $\Delta S = 0$. However, it can occur through spin-orbit coupling and the matrix element of interest,

$$\langle X^1\Sigma^+ | \boldsymbol{\mu} | a^3\Sigma^+ \rangle_{\text{SO}}, \quad (8)$$

will be nonzero.

We add to the molecular Hamiltonian H the Breit–Pauli H^{SO} perturbation term given by¹⁴

$$H^{\text{SO}} = \frac{\alpha^2}{2} \sum_{iA} \frac{Z_A}{r_{iA}^3} \mathbf{l}_{iA} \cdot \mathbf{s}_i - \frac{\alpha^2}{2} \sum_{i \neq j} \frac{1}{r_{ij}^3} (\mathbf{r}_{ij} \times \mathbf{p}_i) \cdot (\mathbf{s}_i + 2\mathbf{s}_j), \quad (9)$$

where i and A denote electrons and nuclei, respectively, and α is the fine structure constant. The first term in Eq. (9) is the direct spin-orbit interaction, while the second term is the spin-other orbit interaction. As this perturbation mixes the spin and orbital angular momenta of the electrons, the correct quantum number is $\Omega = \Lambda + \Sigma$. In this representation, the states characterized by Λ and Σ split into Ω components, whose symmetry can be determined by group theory¹⁵ from the direct product of the spatial and spin symmetry species. The $a^3\Sigma^+$ state will split into two components corresponding to the Π and Σ^- irreducible representations of the $C_{\infty v}$ point group. Using standard labeling, these components are denoted $\Omega = 1$ and $\Omega = 0^-$, respectively. All the $\Omega \neq 0$ components are doubly degenerate. However, the diagonal elements of H^{SO} can be shown to be proportional to $\Lambda\Sigma$ so that the three components of the $^3\Sigma^+$ state are still degenerate.¹⁴

The selection rules for spin-orbit coupling are¹⁶

$$\Delta\Omega = 0; \quad \Delta S = 0, \pm 1; \quad \Delta\Lambda = -\Delta\Sigma = 0, \pm 1; \quad \Sigma^+ \leftrightarrow \Sigma^-. \quad (10)$$

In accordance with the last rule, there will be no spin-orbit interaction between the $a^3\Sigma^+$ and the $^1\Sigma^+$ states. However, if we take into account higher parts of the spectrum of HeH^+ , and in particular Π states, the transition will become possible.

If we consider a $^1\Pi$ and a $^3\Pi$ state, we can use the rules (10) to write the $X^1\Sigma^+$ and $a^3\Sigma^+$ wave functions in the spin-orbit representation in terms of the unperturbed functions as

$$|X^1\Sigma_0^+\rangle_{\text{SO}} = c_1 |X^1\Sigma_0^+\rangle + c_2 |^3\Pi_0^+\rangle,$$

$$|a^3\Sigma_0^+\rangle_{\text{SO}} = c_3 |a^3\Sigma_0^+\rangle + c_4 |^3\Pi_0^-\rangle, \quad (11)$$

$$|a^3\Sigma_1^+\rangle_{\text{SO}} = c_5 |a^3\Sigma_1^+\rangle + c_6 |^1\Pi_1\rangle + c_7 |^3\Pi_1\rangle,$$

where the coefficients c_i are obtained by diagonalizing the spin-orbit matrix in the basis of the unperturbed functions.

The relevant matrix element (8) in the spin-orbit representation can be evaluated, provided that the mixing coefficients and the dipole transition functions are known in the unperturbed basis. Due to the splitting of the triplet state into two components, the matrix element (8) is split into two parts, according to the value of Ω . However, the matrix element $\langle X^1\Sigma_0^+ | \boldsymbol{\mu} | a^3\Sigma_0^+ \rangle$ vanishes identically due to the fact

TABLE I. Molecular states included in the calculations together with their dissociative products and energy at $R=70$ a.u.

Symmetry	$U_{m\Lambda\Sigma}(R=70)$	Dissociative atomic states
$X^1\Sigma^+$	-2.903 243 07	$H^+ + He(1s^2\ ^1S)$
$a^3\Sigma^+$	-2.499 960 40	$H(1s) + He^+(1s)$
$1^1\Pi$	-2.124 916 60	$H(2p) + He^+(1s)$
$2^1\Pi$	-2.123 684 73	$H^+ + He(1s2p\ ^1P^o)$
$3^1\Pi$	-2.056 398 37	$\frac{1}{\sqrt{2}}H(3p) + \frac{1}{\sqrt{2}}H(3d) + He^+(1s)$
$4^1\Pi$	-2.056 164 25	$H^+ + He(1s3d\ ^1D)$
$5^1\Pi$	-2.054 563 33	$\frac{1}{\sqrt{2}}H(3p) - \frac{1}{\sqrt{2}}H(3d) + He^+(1s)$
$1^3\Pi$	-2.132 825 25	$H^+ + He(1s2p\ ^3P^o)$
$2^3\Pi$	-2.124 918 45	$H(2p) + He^+(1s)$
$3^3\Pi$	-2.058 144 10	$H^+ + He(1s3p\ ^3P^o)$

that the electric dipole operator cannot connect 0^+ with 0^- states. The component $a^3\Sigma_0^+$ will thus decay through another mechanism such as spin-rotation or relativistic magnetic dipole perturbations, which are smaller by several orders of magnitude. We will therefore only be able to calculate the lifetime of the $\Omega=1$ component of $a^3\Sigma^+$. However, as the three components are degenerate, the total lifetime of this state will be given by

$$\tau_v^{-1}(a^3\Sigma^+) = \frac{2}{3} \frac{4}{3\hbar^4 c^3} \sum_{v'} E_{vv'}^3 |\langle X^1\Sigma_0^+ v | \boldsymbol{\mu} | a^3\Sigma_1^+ v' \rangle_{SO}|^2. \quad (12)$$

The matrix element (8) can be evaluated for the $\Omega=1$ component using Eq. (11) as

$$\langle X^1\Sigma_0^+ | \boldsymbol{\mu} | a^3\Sigma_1^+ \rangle_{SO} = c_1 c_6 \langle X^1\Sigma^+ | \boldsymbol{\mu} | 1^1\Pi \rangle + c_2 c_5 \langle 3^1\Pi | \boldsymbol{\mu} | a^3\Sigma^+ \rangle + c_2 c_7 \langle 3^1\Pi | \boldsymbol{\mu} | 3^1\Pi \rangle. \quad (13)$$

All the dipole matrix elements occurring in Eq. (13) are non-zero for the μ_x and μ_y components of the dipole operator, and the extension of Eqs. (11) and (13) to the case of more than one singlet or/and triplet Π state is straightforward.

III. RESULTS AND DISCUSSION

A. Dipole transition function

We will consider here the lower part of the spectrum of HeH^+ , which is composed of states that dissociate either into $H^+ + He(1snl\ ^{1,3}L)$ or into $H(nl) + He^+(1s)$. As the various $^1\Sigma^+$ and $^3\Sigma^+$ states cannot interact through spin-orbit perturbation, it is not necessary to include in the spin-orbit calculations other Σ states than the $X^1\Sigma^+$ and the $a^3\Sigma^+$. On the other hand, all the singlet and triplet Π states will contribute to the matrix element (8). We have found (see below) that five $^1\Pi$ and three $^3\Pi$ are sufficient to describe correctly the transition. The states included are given in Table I together with their dissociation products, and their adiabatic potential energy curves are presented in Fig. 1.

All the calculations were done using the MOLPRO program¹⁰ and an adapted basis set which consists for each

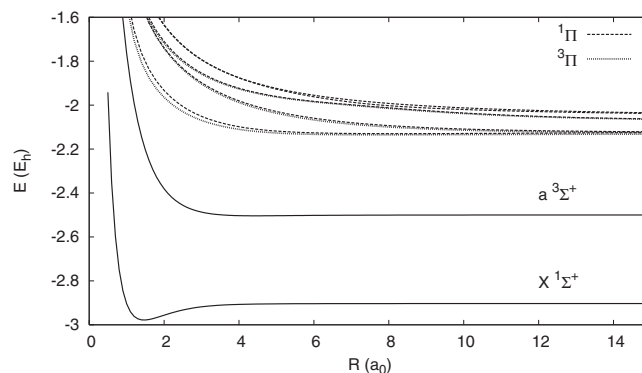
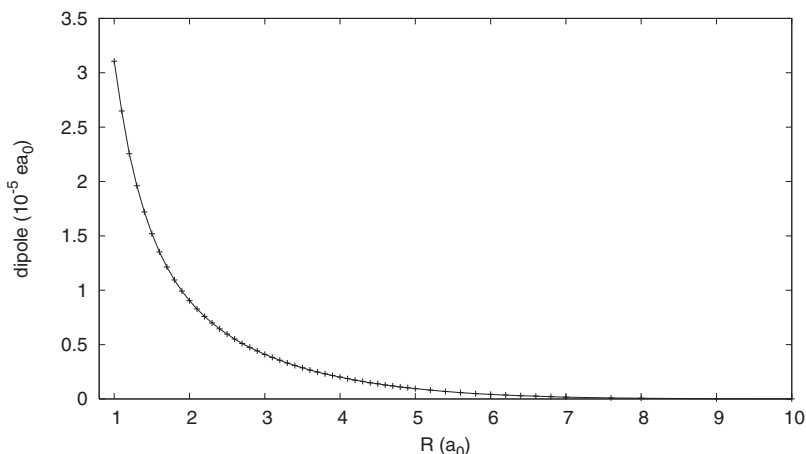


FIG. 1. Potential energy curves of the molecular states included in the calculations.

atom of the aug-cc-pV5Z (or AV5Z) basis set^{17,18} augmented by $[3s, 3p, 2d, 1f]$ Gaussian-type orbitals optimized to reproduce the spectroscopic orbitals of the He and H excited states (see Ref. 19 for details). To obtain the potential energy curves for the electronic states, we performed a state-averaged CASSCF (Refs. 20 and 21) using an active space of five σ , ten π , and one δ orbitals followed by a configuration interaction (CI) calculation. These potential energy curves were already used to describe with success the photodissociation of HeH^+ and the charge transfer process in $H + He^+$ collisions.²² The Breit-Pauli spin-orbit matrix has been calculated on the basis of the unperturbed CASSCF eigenfunctions. To include additional correlation effects, we replaced the CASSCF energies (the diagonal elements of the spin-orbit matrix) by the calculated CI energies. This matrix is then diagonalized using the state interacting method²³ implemented in MOLPRO. The diagonalization of the spin-orbit matrix corresponding to all (Λ, Σ) states of Table I provides 32 roots corresponding to 4, 4, 9, and 3 states with $\Omega=0^+, 0^-, 1,$ and 2 , respectively.

The evolution of the dipole transition moment (8) as a function of the internuclear distance is presented in Fig. 2. It is of order 10^{-5} a.u., in agreement with the fact that the spin-orbit interactions are small in light molecules. It also decreases rapidly, corresponding to the fact that the value of the spin-orbit matrix elements under consideration vanishes in the atomic limit.

In Fig. 3 is presented the weight of each of the Π states taken into account into the dipole matrix element $\langle X^1\Sigma_0^+ v | \boldsymbol{\mu} | a^3\Sigma_1^+ v' \rangle_{SO}$, i.e., the relative contribution of each state to the total dipole transition function. We see that the matrix element is dominated by the contribution from the first $^1\Pi$ state. The inclusion of the second and third $^1\Pi$ states modifies the matrix element by more than 10%, but the fourth and fifth $^1\Pi$ states bring an additional correction of only 2%–3% so that it can be supposed that the inclusion of more singlet Π states will not affect dramatically the lifetime. The contribution of the first triplet Π state increases with the internuclear distance but does not exceed 10%, while the second and third $^3\Pi$ states contribute to less than 3%. It is therefore reasonable to assume that the value of the lifetime obtained when considering five $^1\Pi$ and three $^3\Pi$ states is correct up to a few percent.

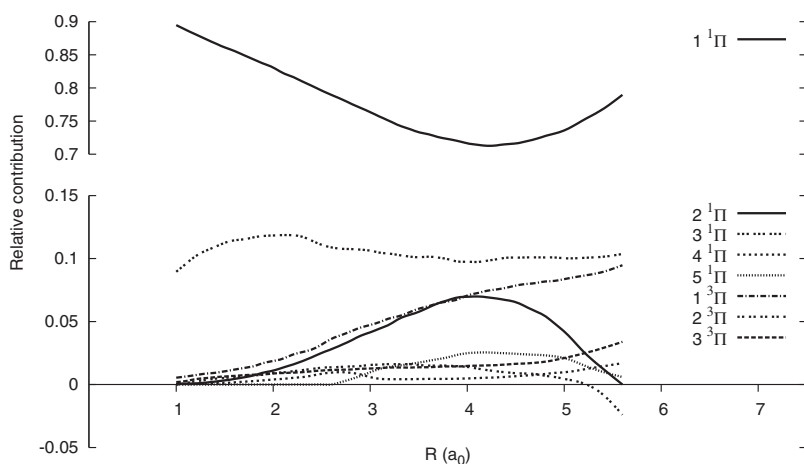
FIG. 2. Dipole transition function $\langle X^1\Sigma_0^+ | \mu | a^3\Sigma_1^+ \rangle_{SO}$.

B. Vibrational analysis of the $X^1\Sigma^+$ and $a^3\Sigma^+$ states

The vibrational analysis of the $X^1\Sigma^+$ and $a^3\Sigma^+$ states was done using a B-spline basis set method.²⁴ The *ab initio* calculation of molecular vibrational spectra involving highly excited vibrational states implies the variational resolution of the purely vibrational Schrödinger equation by analytical finite basis set (FBS) or numerical discrete variable representation (DVR) approaches. In this work, B-spline basis sets are used as alternative FBS method. The flexibility of B-splines has been demonstrated in atomic and molecular calculations^{25,26} by an accurate description of both the bound and the continuum states and their efficiency in the resolution of the nuclear motion of molecules has been assessed. In opposition with the DVR, which is constrained by a uniform distribution of the grid points, the B-splines allow more flexibility from the definition of different cavities in which the number of grid points can be adjusted.

The definition of a B-spline basis set on a cavity of size $L = x_{\max} - x_{\min}$ starts with the definition of a sequence of N real-valued knots $\{t_i\}$, satisfying $t_i \leq t_{i+1}$. Using this knot sequence, a set of N polynomials, all with same degree, is defined: the B-splines of order K (and degree $K-1$). The recursive definition of the B-splines $B_{i,k}(x)$ is the following:

$$B_{i,1}(x) = \begin{cases} 1 & \text{if } t_i \leq x \leq t_{i+1} \\ 0 & \text{otherwise,} \end{cases}$$

FIG. 3. Relative contributions of the five $^1\Pi$ and the three $^3\Pi$ states to the dipole transition function $\langle X^1\Sigma_0^+ | \mu | a^3\Sigma_1^+ \rangle_{SO}$.

$$B_{i,k}(x) = \frac{x - t_i}{t_{i+k-1} - t_i} B_{i,k-1}(x) + \frac{t_{i+k} - x}{t_{i+k} - t_{i+1}} B_{i+1,k-1}(x). \quad (14)$$

It should be mentioned that we are free to choose the order K , the knot sequence, and the interval of the basis set. The space that is spanned by a B-spline depends on this degree; the higher the degree, the larger the space that is spanned. We used B-splines of order 13 on a grid with $x_{\min} = 0.5$ a.u. and $x_{\max} = 100$ a.u. divided by 800 equidistant knot points. These parameters were implemented in a home-made program.²⁷ The accuracy of our results has been assessed by varying the order of the splines, the knot sequence, and the size of the radial grid.

Extensive studies of the ground state of HeH^+ have been done by Kołos and Peek²⁸ or Bishop and Cheung.²⁹ We reproduce the value for the position of the minimum found by these authors, which is 1.463 a.u. Kołos and Peek find a dissociation energy of 16 455.64 cm^{-1} and Bishop and Cheung obtained a value of 16 456.15 cm^{-1} when Born–Oppenheimer diagonal corrections are included. Our result of 16 465.5 cm^{-1} is therefore about 9 cm^{-1} larger. The replacement of the AV5Z by the AV6Z basis set leads to an improvement of less than 2 cm^{-1} .

The vibrational energies of the ground state of HeH^+ have been studied before using diagonal Born–Oppenheimer corrections by Bishop and Cheung,²⁹ or with nonadiabatic and relativistic effects by Stanke *et al.*³⁰ As was found in

TABLE II. Energy difference $E_v - E_{v+1}$ between two successive vibrational levels of the $X^1\Sigma^+$ state of HeH^+ in cm^{-1} and comparison with previous works. Basis 1: AV5Z+adapted basis set; basis 2: AV6Z+adapted basis set.

v	Basis 1	Basis 2	Stanke <i>et al.</i> ^a	Bishop and Cheung ^b
0	2910.40	2910.57	2911.02	2911.29
1	2604.12	2604.13	2604.21	2604.32
2	2296.13	2296.02	2295.64	
3	1983.20	1983.02	1982.13	
4	1662.19	1661.90	1660.45	
5	1330.39	1329.98	1327.91	
6	987.71	987.20	984.50	
7	643.06	642.45	639.35	
8	330.72	330.26	327.49	
9	117.51	117.61	116.22	
10	24.92	24.88	24.44	

^aReference 30.

^bReference 29.

these papers, we obtain 12 vibrational levels. Due to the fact that we have neglected several terms in the Hamiltonian, we do not reproduce the absolute energies of the levels. However, the energy separation between these levels is correct with an error of less than 3 cm^{-1} , as shown in Table II. The effect of diagonal Born–Oppenheimer corrections on the spacing between vibrational levels is less than 1 cm^{-1} while the effect of relativistic corrections is smaller than 0.1 cm^{-1} , as shown by Bishop and Cheung and Stanke *et al.*, respectively. The $v=11$ level, not shown in Table II, has a binding energy of 1.35 cm^{-1} , to be compared with the value of 1.30 cm^{-1} found by Stanke *et al.* It should be noted that the use of the AV6Z instead of the AV5Z basis set leads to different absolute energies for the vibrational levels, but that the spacing remains the same.

The $a^3\Sigma^+$ state has been studied by Michels,³¹ and a more accurate study was done by Kołos³² using variational wave functions in elliptic coordinates. Both authors found the minimum to be located at 4.47 a.u., but the dissociation energy found by Michels is 661.4 cm^{-1} while the result of Kołos is 849.0 cm^{-1} . We find an equilibrium position of 4.452 a.u. and a dissociation energy of 849.79 cm^{-1} .

The only calculations on the vibrational levels of the $a^3\Sigma^+$ state were done using the potential energy curve given by Michels completed by an analytical expression at large R and it was found that this state supports five vibrational levels.⁸ The binding energies of the levels $v=0-3$ can be found in this article and a more recent work³³ in which more precise values are presented. We reproduce the energy of these levels up to 1 cm^{-1} . However, using our potential energy curve we find that this state supports six vibrational levels, with the $v=5$ state being bound by less than 2 cm^{-1} . The total energies are given in Table III, together with the binding energies. While the $v=5$ level has a very small binding energy, it appears as a bound state in all our test calculations: the effect of the variation of B-spline parameters such as the size of the basis set or the grid size did not influence the energy of this state, and the use of the AV6Z basis set only induces a correction of 0.05 cm^{-1} .

The vibrational energies presented in Table III correspond to Hund's case (b) for $J=0$ so that the centrifugal

TABLE III. Total and binding energies of the bound vibrational levels of the $a^3\Sigma^+$ state of HeH^+ as well as the energy difference $E_v - E_{v+1}$ between two successive vibrational levels. Total energies in atomic units, binding energies in cm^{-1} .

v	E_{tot}	E_{bind}	$E_v - E_{v+1}$
0	-2.502 969 82	-664.834	297.67
1	-2.501 613 56	-367.169	199.92
2	-2.500 702 66	-167.249	109.99
3	-2.500 201 52	-57.260	44.61
4	-2.499 998 26	-12.652	11.53
5	-2.499 945 75	-1.126	
Unbound	-2.499 940 62		

correction in Eq. (4) vanishes. As we have seen, we will only be able to calculate the lifetime of the $\Omega=1$ components of the $a^3\Sigma^+$ state. For these, the centrifugal term also vanishes [see Eq. (4)], so that the vibrational energies presented in Table III are still valid.

C. Calculation of the lifetime

As can be seen from Eq. (7), the Einstein coefficients will depend on the dipole matrix element between the initial and final electronic states, and on the overlap of the vibrational functions. We have seen that the dipole is very small, but in addition the overlap of the vibrational functions is small since the two states under consideration have their minima located at very different geometries, as illustrated in Fig. 4.

Using the B-splines, it is a simple task to integrate the overlap between the vibrational functions, multiplied by the

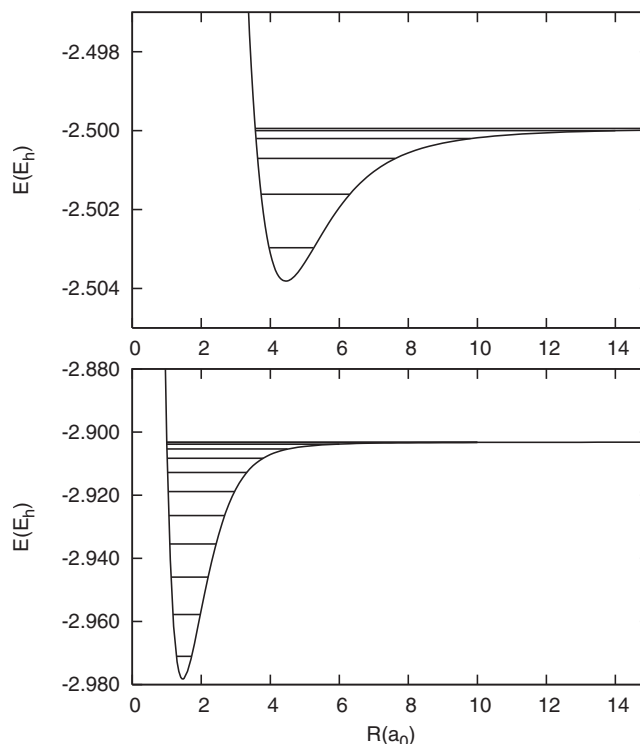


FIG. 4. Adiabatic potential energy curves of the first triplet $a^3\Sigma^+$ state (above) and of the ground $X^1\Sigma^+$ state (below) of HeH^+ and position of the bound vibrational levels supported by these states.

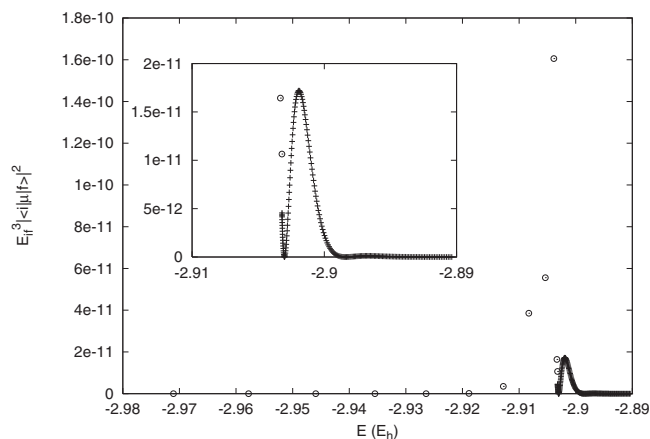


FIG. 5. Contribution from the discrete (circles) and continuum (crosses) parts of the vibrational spectrum to the Einstein coefficients A_{if} for $v_i=1$ as a function of the energy of the final vibrational levels.

R -dependent dipole matrix element. We performed the integration on a grid $R \in [1, 100]$. For the continuum part of the spectrum, it is necessary to sum over all vibrational functions of the pseudocontinuum spectrum until convergence.

In Fig. 5 are presented the contributions from the discrete and continuum parts of the vibrational spectrum to the Einstein coefficients A_{if} . It is seen that the convergence is reached with 200 continuum functions. To represent this contribution, it is necessary to take into account the fact that the vibrational continuum has been discretized by multiplying the A_{if} by the density of states $\rho(E)=2/(E(v_{f+1})-E(v_{f-1}))$. For the discrete part of the spectrum, there is no density of states, but the A_{if} should still be multiplied by some value to allow comparison since $\rho(E)$ depends on the energy units we choose. Following Ref. 33, we use a density for the bound states given by $\rho(E)=1/(E(v_{f+1})-E(v_f))$. In Fig. 5, we observe the continuity of the results around the dissociation limit.

The lifetime, as well as the relative contribution from bound and continuum states, is presented in Table IV. We observe that the lifetime increases with the vibrational number v . We also see that the contribution of the continuum to the lifetime is very small (5%) for $v_i=0$, but increases with the value of v_i up to 30% for $v_i=5$. The contribution of the higher lying Π states will probably reduce the lifetime by a few percent, but our calculations provide an upper bound of 150 s on the lifetime of the $v=0$ level of the $a^3\Sigma^+$ state in the absence of collisional decay.

TABLE IV. Relative contributions of the discrete and of the continuum parts of the vibrational spectrum to the sum of the Einstein coefficients A_{if} and value of the lifetime of the $\Omega = \pm 1$ component of $a^3\Sigma^+$ for $v_i=0-5$.

v_i	Bound	Continuum	Lifetime (s)
0	0.949	0.051	149
1	0.906	0.094	211
2	0.786	0.214	347
3	0.709	0.291	738
4	0.694	0.306	2288
5	0.692	0.308	14 267

IV. CONCLUSIONS

We have determined the radiative lifetime of the $a^3\Sigma^+$ state of HeH^+ using *ab initio* methods. The decay of this state onto the ground $X^1\Sigma^+$ state is spin-forbidden but can occur through spin-orbit coupling. We took into account the interaction of the $a^3\Sigma^+$ and $X^1\Sigma^+$ states with the first five $^1\Pi$ and three $^3\Pi$ states of HeH^+ to estimate the dipole transition matrix element $\langle X^1\Sigma^+ | \mu | a^3\Sigma^+ \rangle_{\text{SO}}$. The vibrational energies and wave functions of the $a^3\Sigma^+$ and $X^1\Sigma^+$ states were obtained using a B-spline method and were found to agree well with previous calculations. We presented theoretical values of the lifetime of the six vibrational levels of the $a^3\Sigma^+$ state. The lifetime is found to be of about 150 s for the $v=0$ state and increases rapidly with v , as does the contribution of the continuum states to the lifetime. Such a long lifetime suggests that HeH^+ could be present in the $a^3\Sigma^+$ state in astrophysical environments. We will investigate the radiative association in this state in a separate work.

ACKNOWLEDGMENTS

J. Loreau would like to thank the FRIA for financial support. This work was supported by the Fonds National de la Recherche Scientifique (IISN projects) and by the Action de Recherche Concertée ATMOS de la Communauté Française de Belgique.

- S. Lepp, P. C. Stancil, and A. Dalgarno, *J. Phys. B* **35**, R57 (2002).
- J. H. Black, *Astrophys. J.* **222**, 125 (1978).
- G. J. Harris, A. E. Lynas-Gray, S. Miller, and J. Tennyson, *Astrophys. J.* **617**, L143 (2004).
- J. M. Moorhead, R. P. Lowe, J.-P. Maillard, W. H. Wehlau, and P. F. Bernath, *Astrophys. J.* **326**, 899 (1988).
- X.-W. Liu, M. J. Barlow, A. Dalgarno, J. Tennyson, T. Lim, B. M. Swinyard, J. Cernicharo, P. Cox, J.-P. Baluteau, D. Péquignot, Nguyen-Q-Rieu, R. J. Emery, and P. E. Clegg, *Mon. Not. R. Astron. Soc.* **290**, L71 (1997).
- T. R. Hogness and E. C. Lunn, *Phys. Rev.* **26**, 44 (1925).
- W. Roberge and A. Dalgarno, *Astrophys. J.* **255**, 489 (1982).
- F. B. Yousif, J. B. A. Mitchell, M. Rogelstad, A. Le Paddelec, A. Canosa, and M. I. Chibisov, *Phys. Rev. A* **49**, 4610 (1994).
- D. Strasser, K. G. Bhushan, H. B. Pedersen, R. Wester, O. Heber, A. Lafosse, M. L. Rappaport, N. Altstein, and D. Zajfman, *Phys. Rev. A* **61**, 060705 (2000).
- MOLPRO, a package of *ab initio* programs designed by H.-J. Werner and P. J. Knowles, Version 2006.1, R. Lindh, F. R. Manby, M. Schütz *et al.*
- M. R. Manaa and D. R. Yarkoni, *J. Chem. Phys.* **95**, 6562 (1991).
- P. Palmieri, R. Tarroni, G. Chambaud, and P. Rosmus, *J. Chem. Phys.* **99**, 456 (1993).
- J. Oddershede, *Phys. Scr.* **20**, 587 (1979).
- H. Lefebvre-Brion and R. W. Field, *The Spectra and Dynamics of Diatomic Molecules* (Elsevier Academic, Amsterdam, 2004).
- G. Herzberg, *Electronic Spectra of Polyatomic Molecules* (Van Nostrand, New Jersey, 1966).
- K. Kayama and J. C. Baird, *J. Chem. Phys.* **46**, 2604 (1967).
- T. H. Dunning, *J. Chem. Phys.* **90**, 1007 (1989).
- D. E. Woon and T. H. Dunning, *J. Chem. Phys.* **100**, 2975 (1994).
- J. Loreau, P. Palmeri, P. Quinet, J. Liévin, and N. Vaeck, *J. Phys. B* **43**, 065101 (2010).
- H.-J. Werner and P. J. Knowles, *J. Chem. Phys.* **82**, 5053 (1985).
- P. J. Knowles and H.-J. Werner, *Chem. Phys. Lett.* **115**, 259 (1985).
- K. Sodoga, J. Loreau, D. Lauvergnat, Y. Justum, N. Vaeck, and M. Desouter-Lecomte, *Phys. Rev. A* **82**, 033417 (2009); J. Loreau, K. Sodoga, D. Lauvergnat, M. Desouter-Lecomte, and N. Vaeck, *Phys. Rev. A* **82**, 012708 (2010).
- A. Berning, M. Schweizer, H.-J. Werner, P. J. Knowles, and P. Palmieri, *Mol. Phys.* **98**, 1823 (2000).

- ²⁴C. de Boor, *A Practical Guide to Splines* (Springer-Verlag, New York, 1978).
- ²⁵B. W. Shore, *J. Phys. B* **6**, 1923 (1973).
- ²⁶H. Bachau, E. Cormier, P. Decleva, J. E. Hansen, and F. Martin, *Rep. Prog. Phys.* **64**, 1815 (2001).
- ²⁷A. Dian, Ph.D. thesis, ULB, 2002.
- ²⁸W. Kołos and J. M. Peek, *Chem. Phys.* **12**, 381 (1976).
- ²⁹D. M. Bishop and L. M. Cheung, *J. Mol. Spectrosc.* **75**, 462 (1979).
- ³⁰M. Stanke, D. Kedziera, M. Molski, S. Bubin, M. Barysz, and L. Adamowicz, *Phys. Rev. Lett.* **96**, 233002 (2006).
- ³¹H. H. Michels, *J. Chem. Phys.* **44**, 3834 (1966).
- ³²W. Kołos, *Int. J. Quantum Chem.* **10**, 217 (1976).
- ³³M. I. Chibisov, F. B. Yousif, P. J. T. Van der Donk, and J. B. A. Mitchell, *Phys. Rev. A* **54**, 4997 (1996).